Large-Scale Fe_3O_4 Nanoparticles Soluble in Water Synthesized by a Facile Method

Chao Hui, Chengmin Shen, Tianzhong Yang, Lihong Bao, Jifa Tian, Hao Ding, Chen Li, and H.-J. Gao*

Beijing National Laboratory for Condensed Matter Physics, Institute of Physics, Chinese Academy of Sciences, Beijing 100080, People's Republic of China

Received: February 25, 2008; Revised Manuscript Received: April 29, 2008

Large-scale hydrophilic Fe_3O_4 nanoparticles (NPs) were prepared in the presence of citrate and sodium nitrate via a facile method. The Fe_3O_4 NPs are quite stable and can be freely dispersed in water. The as-prepared magnetic nanoparticle solution can be stable for more than 1 month. The mean diameter of the Fe_3O_4 NPs can be controlled in the range of ~20 to ~40 nm in mean diameter. The NPs show superparamagnetic properties with a relatively high saturation magnetization moment 58 emu/mg at room temperature. Furthermore, a possible formation mechanism is proposed to explain why the magnetic nanoparticles are very well soluble in water.

Introduction

The synthesis of transition metals and their oxide nanoparticles (NPs) is of importance in nanotechnology research due to their potential and practical applications.[1–6] Among the materials, magnetite (Fe_3O_4) is a common magnetic iron oxide that has a cubic inverse spinel structure with oxygen forming a face-centered cubic closed packing and iron cations occupying interstitial tetrahedral sites and octahedral sites.[7] Fe_3O_4 NPs have raised up much interest in the field of information storage as well as the areas of biomedicine and magnetic sensing.[8–10] Especially, Fe_3O_4 NPs are reported to be applicable for drug delivery systems (DDS), magnetic resonance imaging (MRI), and cancer therapy.[11–13] Because of the strong need for high-density storage, the synthesis and characterization of magnetic NPs have been extensively investigated.[14–17] Chemical methods for preparing magnetic iron oxide NPs are mainly divided into two routes: (1) thermal decomposition of iron organometallic compounds in a higher boiling point organic solvent and (2) coprecipitation in aqueous solution using polymer or charged molecules as surfactants. Magnetite NPs synthesized in organic solvent are energy-intensive, employ toxic chemicals, and yield NPs in nonpolar solutions.[18] These properties do not facilitate the magnetite NPs' biomedical applications. In contrast, biological synthesis of magnetite NPs occurs in water at room temperature and the pH value is close to neutral.[19] Hydrophilic NPs, which are useful in biochemistry, must be soluble in water in a pH range of about 5−9.[20] Therefore, a high dispersity in water is of great importance for biology-related applications.

In this article, we reported on a facile method to synthesize Fe_3O_4 NPs with a high dispersity and a high stability in water. The size of Fe_3O_4 NPs can be controlled by tuning reaction conditions. The morphology and magnetic properties of the NPs have been investigated. This method is suitable for preparation of Fe_3O_4 NPs on the gram scale.

Experimental Section

Synthesis. A typical synthesis of hydrophilic magnetite NPs is as follows: 1 mmol of $C_6H_5Na_3O_7 \cdot 2H_2O$ (citric acid, trisodium salt dehydrate), 4 mmol of NaOH, and 0.2 mol of $NaNO_3$ are mixed in 19 mL of deionized water. The mixture was then heated to 100 °C and formed a pellucid solution. 1 mL of 2 M $FeSO_4 \cdot 4H_2O$ (2mmol) solution was added into the mixture rapidly (equivalent to 0.10 M Fe^{2+} in the alkali solution), and the mixed solution was kept at 100 °C for 1 h. The solution was then cooled down to room temperature naturally. The Fe_3O_4 NPs were separated and purified from solvent by a magnet for several times. A black precipitation was obtained and then redissolved in water by an ultrasonic water bath for several minutes. The diameter of Fe_3O_4 NPs can be controlled in the range of ~20 to ~40 nm by varying the experimental parameters. The as-synthesized NPs with a mean diameter of 20 nm are stable in water for at least one month. The NPs can be redispersed in water even after dried into a powder for several weeks.

Characterization. The structure of hydrophilic NPs was characterized by using a Mac Science M18AHF X-ray Diffraction with Cu Kα radiation (1.5418Å) generated at 40 kV and 30 mA. The surface of Fe_3O_4 NPs was measured by using a VG ESCALAB-5 X-ray photoelectron spectrometry (XPS) system. To identify the presence of citrate on the NPs' surface, FTIR spectra was measured by using a BRUKER VECTOR 22 Fourier transform infrared spectrometer. Transmission electron microscopy (TEM) images and electron diffraction (ED) patterns of the NPs were obtained by a JEOL 200CX microscope operated at an acceleration voltage of 120 kV. The nanoparticle powder samples were dispersed in ultra pure water by sonication and then dropped onto a copper grid for TEM observation. The size distribution of NPs was determined by measuring diameters of one hundred NPs randomly selected on the TEM images. Magnetic properties of powder samples were characterized with a Quantum Design PPMS 6000 by measuring the applied field dependence of magnetization between −14 and 14 kOe at 300 K.

Results and Discussion

Gram-scale well-soluble hydrophilic Fe_3O_4 NPs were prepared by using a facile one-step method. This route gave a gram scale of hydrophilic Fe_3O_4 NPs that can be redispersed in water. Figure 1 shows samples of solid state hydrophilic Fe_3O_4 NPs

* To whom correspondence should be addressed. Phone: 86-10-82648035. Fax: 86-10-62556598. Email: hjgao@aphy.iphy.ac.cn.

10.1021/jp801632p CCC: $40.75
Published on Web 07/09/2008

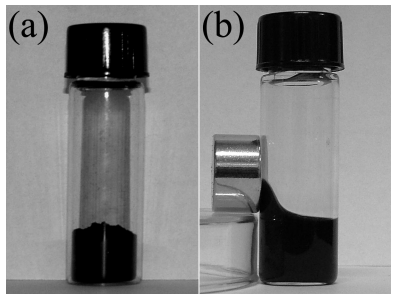

Figure 1. Gram-scale well-soluble hydrophilic Fe_3O_4 NPs were prepared by using a facile one-step method. (a) Samples of solid state hydrophilic Fe_3O_4 NPs powder. (b) Dispersion in water, which can be moved by a magnet.

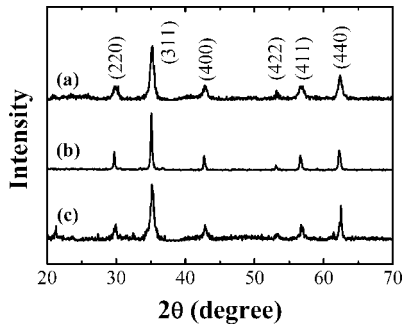

Figure 2. XRD patterns of (a) as-synthesized 20-nm Fe_3O_4 NPs and (b) as-synthesized 40-nm Fe_3O_4 NPs, which show the cubic inverse spinel structure of the sample. (c) XRD pattern of 20-nm Fe_3O_4 NPs kept in air for 3 months. All samples were deposited on glass substrates from their water dispersions.

powder and the solution obtained after dispersed in water. Figure 1b shows that the dispersion is a kind of magnetic fluid that can be attracted by an external magnet. And the dispersion can be stable for more than one month as the NPs have good dispersity and high stability in water.

Figure 2 shows X-ray diffraction (XRD) patterns of Fe_3O_4 NPs that indicated a highly crystalline cubic spinel structure of Fe_3O_4. Parts a and b of Figure 2 show the XRD patterns of two different-sized Fe_3O_4 NPs with the diameters of 20 and 40 nm, respectively. The diffraction peaks at 30, 35.4, 43, 53.4, 56.9, and 62.5° responded to [220], [311], [400], [422], [511], and [440] planes of cubic Fe_3O_4 lattice, respectively. These results are in good agreement with those XRD patterns of Fe_3O_4 NPs reported in the literature,[21–25] which confirms the cubic spinel structure of the magnetite materials. The average sizes of the Fe_3O_4 NPs obtained from the calculation of Sherrer's formula based on fwhm (full width at half-maximum) of the major diffraction peaks observed in parts a and b of Figure 2, which are about 20 and 40 nm, respectively. They are consistent with the result of the TEM analysis. It can be concluded that the particles are nearly single crystals.[26,27] The hydrophilic Fe_3O_4 NPs solution has good stability in the air atmosphere. Figure 2c shows XRD pattern of 20nm Fe_3O_4 NPs kept in air for 3 months. In comparison with Figure 2a, few weak diffraction peaks of Fe_2O_3 appeared and the major diffraction peaks have matched with peaks of Fe_3O_4 NPs, indicated that hydrophilic Fe_3O_4 NPs solution were not oxidized in the air.

To understand the surface of hydrophilic Fe_3O_4 NPs, we recorded XPS images areof the Fe_3O_4 NPs, which are shown in Figure 3. From all spectra in Figure 3a, the peaks of the C_{1s}, O_{2p}, and Fe_{2p} were observed, indicating the citrate molecules are located on the surface of NPs. In Figure 3b, Fe shows double peaks with binding energies of 710.4 and 723.2 eV, corresponding to $Fe_{2p3/2}$ and $Fe_{2p1/2}$, respectively. These results are consistent with the values reported for Fe_3O_4 in the handbook.[28]

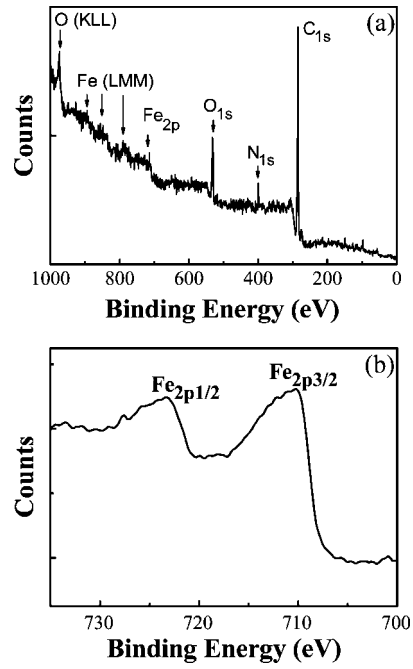

Figure 3. (a) XPS of the as-synthesized magnetite NPs. Evidence for the existence of the organic coating can be found. (b) The details of the iron Fe $_{2p1/2}$ and Fe $_{2p3/2}$ peaks, which match well with the standard data from the handbook.[28]

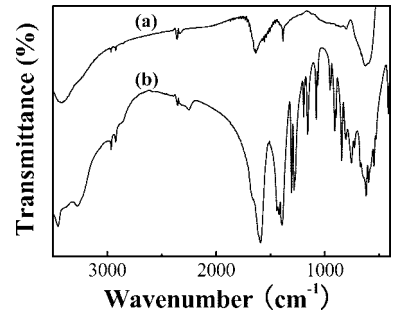

Figure 4. FTIR spectra of citrate-capped Fe_3O_4 NPs (a) and pure $C_6H_5Na_3O_7 \cdot 2H_2O$ (b).

To further investigate information of the surface of citrate-capped Fe_3O_4 nanoparticles, the FTIR spectra of citrate and citrate-capped Fe_3O_4 NPs were measured. The results are shown in Figure 4. It can be clearly observed from parts a and b of Figure 4 that the FTIR spectrum of Fe_3O_4 (Figure 4a) NPs is similar to the spectrum of pure citrate (Figure 4b). Corresponding to peaks of stretching mode ν(as,COO^-) and ν(s,COO^-) of citrate appeared at 1630 cm^{-1} and 1385 cm^{-1} observed in parts a and b of Figure 4, respectively, it indicates that the citrate molecules have been adsorbed on the surface of NPs. However, a remarkable difference in the peak intensity is found between the peaks in Figure 4. The reason for the intensity difference between the two spectra is probably because the citrate on the NPs form a relatively close-packed layer and molecular motion is constrained[4,29,30] Furthermore, the peaks of ν(as,$-CH_2-$) and ν(s, $-CH_2-$) at 2970 cm^{-1} and 2925 cm^{-1} can also be observed in both parts a and b of Figure 4, respectively. These results suggest that citrate is indeed an essential component of the composite.

TEM was used to examine the difference of nanoparticle size. Figure 5 shows the TEM images of various size Fe_3O_4 NPs

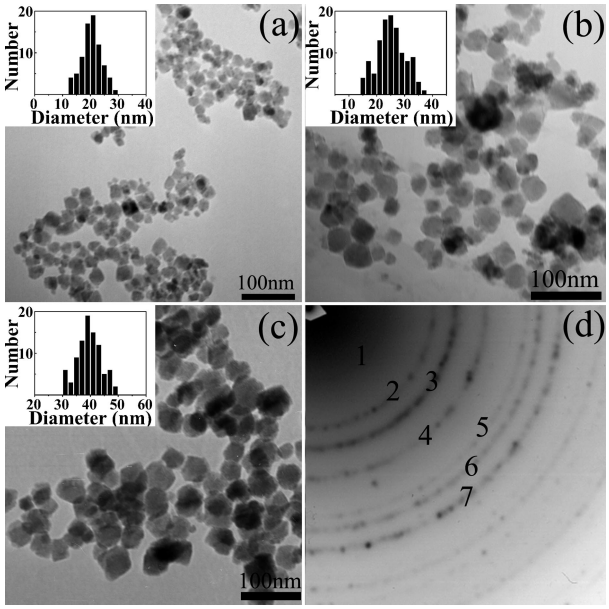

Figure 5. (a, b, c) TEM images and size distributions of Fe_3O_4 NPs with the different mean diameters of 20 (a, $\sigma = 16\%$), 25 (b, $\sigma = 19\%$), and 40 nm (c, $\sigma = 10\%$). The size distributions show that the synthesized Fe_3O_4 NPs had a narrow size distribution. (d) ED patterns of the 20-nm Fe_3O_4 NPs.

TABLE 1: Measured Lattice Spacing, *d* (Å), Based on the ED (Figure 5d)

	1	2	3	4	5	6	7
d	4.85	2.98	2.54	2.08	1.70	1.60	1.47
Fe_3O_4	4.86	2.97	2.53	2.10	1.71	1.62	1.48
hkl	(111)	(220)	(311)	(400)	(422)	(511)	(440)

prepared at different reaction condition. The sizes of Fe_3O_4 NPs ranging from 20 to 40 nm were obtained. TEM images in Figure 5 indicated that the particle size can be controlled by varying the experimental parameters. The size distributions were evaluated by measuring the diameter of more than one hundred NPs randomly selected from the TEM images. The histograms inset of parts a and c of Figure 5 show that the as-synthesized Fe_3O_4 NPs had a narrow size distribution, and the mean diameters of the samples in parts a−c of Figure 5 and were ~20 ($\sigma = 16\%$), ~25 ($\sigma = 19\%$), and ~40 nm ($\sigma = 10\%$), respectively. Additionally, the selected area electron diffraction (SAED) pattern of the 20-nm Fe_3O_4 NPs exhibiting a magnetite structure is shown in Figure 5d. Table 1 shows the measured lattice spacing based on the rings in the electron diffraction pattern (Figure 5d), and the result is in accordance with the known lattice spacing for bulk Fe_3O_4 along with their respective *hkl* indexes from the PDF database.[23]

The magnetic properties of these hydrophilic Fe_3O_4 NPs with an average diameter of 20 nm were measured using a physical property measurement system (PPMS) at room temperature. The hysteresis loop of 20-nm citrate-capped Fe_3O_4 NPs is shown in Figure 6. The hysteresis loop of the Fe_3O_4 nanoparticle powder measured at room temperature shows the expected magnetic behavior. The magnetite NPs does not display magnetic remanence, and the initial slopes of the magnetization curve steeply. These facts are related to finite-size and surface effects. Thus, the NPs are considered to be superparamagnetic. The steep initial slopes show promising applications in nanoscale magnetic devices. The Ms (saturation magnetization) of 20-nm citrate-capped Fe_3O_4 nanoparticles is about 58 emu/g, which is in agreement with the data from the literature.[23] The difference

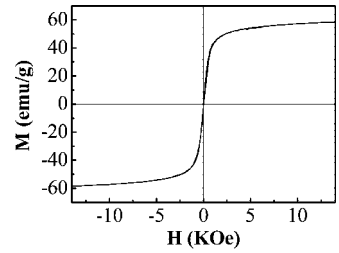

Figure 6. Hysteresis loop measured at 300 K for the 20-nm citrate-capped Fe_3O_4 NPs. The NPs show superparamagnetic properties at room temperature and the M_s is about 58 emu/g.

may come from the dipolar interactions among the NPs, the different particle sizes, the spacing among the NPs, and the characters of the surfactant.

The dispersity and stability in water is an important issue for the magnetic NPs' biomedicine applications. Since the NPs is soluble in water but cannot be dissolved in alcohol, the charge of the citrate ions as surfactant plays a key role. There are three carboxyl groups in every citrate ion, and the repulsive forces between the electric charges of the radical ions make the NPs more dispersed in water. At the same time, if mass of $NaNO_3$ was added into the reactive solution, the ionic strength was highly increased. This increase of ionic strength makes the charges of the NPs surround with citric acid radical equally distributed. Furthermore, some results indicated that the presence of a large amount of salt changes the solubility of organic molecules,[31–33] which is consistent with the Hofmeister Series.[34] It is said that the presence of anion with bigger hydrated ion radius will steady the water−oil interface and then increase the solubility between water and surfactant. Pileni's group also found that, in colloidal solution, addition of anions makes the solubility of surfactant increase to reach a zone in which it is higher than that obtained in pure aqueous solution (salting in).[35–37] That means the water molecules are highly bound to the surfactant. Then the dispersity and stability can be enhanced so as the NPs can be soluble in water and the NPs can be stable for several months. We have also explored that among these different-sized NPs, the 20-nm particles have the best stability in water.

The sizes of magnetite NPs can be controlled in the range of ~20 to ~40 nm in mean diameter by varying the experimental parameters. The average diameter of citrate-capped magnetite NPs depends strongly on the Ostwald Ripening process. So the key to control the sizes of the NPs is to tune the competition between nucleation and growth. When the growth ratio of seeds is larger than one's nucleation ratio, the sizes of the magnetite NPs will be larger or else the sizes will be smaller. Refait and Olowe reported the alkalization reaction of ferrous ions in regard to the formation of iron hydroxide and iron oxide, and they proposed the following reactions as the mechanism of formation of Fe_3O_4 in medium[38,39]

$$Fe^{2+} + 2OH^- \rightarrow Fe(OH)_2 \quad (1)$$

$$3Fe(OH)_2 + 1/2O_2 \rightarrow Fe(OH)_2 + 2FeOOH + H_2O \quad (2)$$

$$Fe(OH)_2 + 2FeOOH \rightarrow Fe_3O_4 + 2H_2O \quad (3)$$

Thus, it is concluded that in the synthesis with ferrous ions alone, Fe_3O_4 is formed as a result of the dehydration reaction of ferrous hydroxide and ferric hydroxide represented by eq 3, in which the latter compound is produced by the partial oxidation of ferrous hydroxide by O_2 dissolved in water according to eq 2. The formation of $Fe(OH)_2$ would be the first process of the

synthesis. We found that a transition temperature of $Fe(OH)_2$ to Fe_3O_4 would be 60 °C. Under this temperature the reaction in eqs 2 and 3 would be completed instantly. So we can change the experimental parameters in eq 1 to control the sizes of the Fe_3O_4 NPs.

To better understand the process of nucleation and growth of Fe_3O_4 in solution, we investigated the influence of experimental conditions on their size and shape. It was found that the three experimental parameters which affect on the size and shape of Fe_3O_4 NPs: (1) the reacting time; (2) the concentration of Fe^{2+} ions, and (3) the amount of $NaNO_3$.

It was also found that the concentration of the Fe^{2+} ions is a key factor for controlling Fe_3O_4 NPs' sizes. A decrease of ferrous precursor concentration from 0.1 to 0.02 M allowes an increase of the average size from 20 to 40 nm; for example, a mean diameter of about 20 nm NPs were prepared by using 0.10 M Fe^{2+} solution. If the concentration of the Fe^{2+} ions was decreased to 0.05 and 0.02 M, 25- and 40-nm Fe_3O_4 NPs would be obtained. The reason for this is that concentration of ferrous precursors strongly affect on nucleation and growth rate of Fe_3O_4 particles. The higher initial precursor concentration leads to smaller particles size due to the formation of a large number of seeds, which provides high particle concentration and yielded small particles.[40]

The higher ionic strength in the solution can affect on the size of NPs as well. It was found that the hydrophilic magnetite NPs with good dispersity were prepared in a saturated solution for 1 h. $NaNO_3$ is a kind of inert activity salt and can be used to make an increase of ionic strength of solution, which will slow the growth and nucleation rate at the same time based on the decrease of the activity of precursor ions. For example, the diameter of 20-nm Fe_3O_4 particles was obtained in 10 M $NaNO_3$, while the size of 40-nm particles can be formed without $NaNO_3$. Furthermore, prolonging the reaction time led to shape of NP more regular. The size of Fe_3O_4 NPs decreased with increasing reaction time. The NPs trended to be more regular when the reaction time was over 1 h.

Conclusions

We have prepared stable citrate-capped Fe_3O_4 nanoparticles soluble in water by using a facile one-step method. This solution can be stable for more than one month in air. The size of Fe_3O_4 NPs was controlled in the range of ~20 to ~40 nm in mean diameter. The NPs are soluble in water depending on the charges of the citric acid on their surface. The NPs show superparamagnetic properties at room temperature. The dispersity and magnetic properties induced by surface and finite-size effects suggest a promising future of the NPs in practical applications.

Acknowledgment. The project is supported by the National Nature Science Foundation of China (Grant No. 60571045), National "863" (2007AA03Z305), and the Key Technologies Research and Development program of China (2003BA310A25).

References and Notes

(1) Sun, S. H.; Murray, C. B.; Weller, D.; Folks, L.; Moser, A. *Science* **2000**, *287*, 1989.

(2) Boal, A. K. In *Synthesis and Applications of Magnetic Nanoparticles in Nanoparticles: Building Blocks for Nanotechnology*; Rotello, V. M., Ed.; Kluwer: New York, 2004; p 1.

(3) Shen, C. M.; Su, Y. K.; Yang, H. T.; Yang, T. Z.; Gao, H. J. *Chem. Phys. Lett.* **2003**, *373*, 39–45.

(4) Johnson, B. K.; Prud'homme, R. K. *Phys. Rev. Lett.* **2003**, *91*, 118302.

(5) Yang, H. T.; Shen, C. M.; Su, Y. K.; Yang, T. Z.; Gao, H. J.; Wang, Y. G. *Appl. Phys. Lett.* **2003**, *82*, 4729–4731.

(6) Chen, M.; Kim, J.; Liu, J. P.; Fan, H.; Sun, S. H. *J. Am. Chem. Soc.* **2006**, *128*, 7132–7133.

(7) Cornell, R. M.; Schwertmann, U. *The Iron Oxides: Structure, Properties, Reactions, Occurrence and Uses*; VCH: New York, 1996, pp 28−29.

(8) Pankhurst, Q. A.; Connolly, J.; Jones, S. K.; Dobson, J. *J. Phys. D: Appl. Phys.* **2003**, *36*, R167.

(9) Sun, S. H.; Zeng, H. *J. Am. Chem. Soc.* **2002**, *124*, 8204–8205.

(10) Sun, S. H. *Adv. Mater.* **2006**, *18*, 393.

(11) Neuberger, T.; Schöpf, B.; Hofmann, H.; Hofmann, M.; von Rechenberg, B. *J. Magn. Magn. Mater.* **2005**, *293*, 483.

(12) Portet, D.; Denizot, B.; Rump, E.; Lejeune, J. J.; Jallet, P. *J. Colloid Interface Sci.* **2001**, *238*, 37.

(13) Iida, H.; Takayanagi, K.; Nakanishi, T.; Osaka, T. *J. Colloid Interface Sci.* **2007**, *314*, 274.

(14) Woo, K. G.; Hong, J. W.; Choi, S. M.; Lee, H. W.; Ahn, J. P.; Kim, C. S.; Lee, S. W. *Chem. Mater.* **2004**, *16*, 2814.

(15) Mallinson, J. C. *The Foundations of Magnetic Recording*; Academic: Berkeley, 1987; Chapter 3.

(16) Bradley, F. N. *Materials for Magnetic Functions*; Hayden: New York, 1976; Chapter 2.

(17) Willner, I.; Patolsky, F.; Wasserman, J. *Angew. Chem., Int. Ed.* **2001**, *40*, 1861.

(18) Hyeon, T. *Chem. Commun.* **2003**, 927–934.

(19) Bharde, A.; Wani, A.; Shouche, Y.; Joy, P. A.; Prasad, B. L. V.; Sastry, M. *J. Am. Chem. Soc.* **2005**, *127*, 9326.

(20) Robinson, D. B.; Persson, H. H. J.; Zeng, H.; Li, G.; Pourmand, N.; Sun, S. H.; Wang, S. X. *Langmuir* **2005**, *21*, 3096–3103.

(21) Maoz, R.; Frydman, E.; Cohen, S. R.; Sagiv, J. *Adv. Mater.* **2000**, *12*, 424.

(22) Stephen, F.; Hakan, R.; Nagaraja, R. S.; Donald, F. *Chem. Mater.* **2002**, *14*, 3643.

(23) Sun, S. H.; Zeng, H.; Robinson, D. B.; Raoux, S.; Rice, P. M.; Wang, S. X.; Li, G. X. *J. Am. Chem. Soc.* **2004**, *126*, 273.

(24) Kim, T. Y.; Lee, M. S.; Kim, Y. I.; Lee, C. S.; Park, J. C.; Kim, D. *J. Phys. D: Appl. Phys.* **2003**, *36*, 1451.

(25) Harris, L. A.; Goff, J. D.; Carmichael, A. Y.; Riffle, J. S.; Harburn, J. J.; St.Pierre, T. G.; Saunders, M. *Chem. Mater.* **2003**, *15*, 1367.

(26) Yang, T. Z.; Shen, C. M.; Li, Z. A.; Zhang, H. R.; Xiao, C. W.; Chen, S. T.; Xu, Z. C.; Shi, D. X.; Li, J. Q.; Gao, H. J. *J. Phys. Chem. B.* **2005**, *109*, 23233.

(27) Yang, T. Z.; Shen, C. M.; Yang, H. T.; Xiao, C. W.; Xu, Z. C.; Chen, S. T.; Shi, D. X.; Gao, H. J. *Surf. Interface Anal.* **2006**, *38*, 1063–1067.

(28) Moudler, J. F.; Stickle, W. F.; Sobol, P. E.; bonben, K. D. *Handbook of X-ray photoelectron spectroscopy*; Perkin-Elmer: Eden Prairie, MN, 1992.

(29) Korgel, B. A.; Fullam, S.; Connolly, S.; Fitzmaurice, D. *J. Phys. Chem. B* **1998**, *102*, 8379.

(30) Lu, Z. L.; Zou, W. Q.; Lv, L. Y.; Liu, X. C.; Li, S. D.; Zhu, J. M.; Zhang, F. M.; Du, Y. W. J. *Phys. Chem. B* **2006**, *110*, 23817.

(31) Collins, K. D.; Washabaugh, M. *Rev. Biophys.* **1985**, *18*, 323.

(32) Franks, K. In *Waters A Comprehensive Treatise*; Plenum: New York, 1973; Vol. 2, p 1.

(33) Eagland, D. In *Waters A Comprehensive Treatise*; Plenum: New York, 1973; Vol. 4, p 305.

(34) Hofmeister, F. *Arch. Exp. Pathol. Pharmakol.* **1888**, *24*, 247.

(35) Filankembo, A.; Giorgio, S.; Lisiecki, I.; Pileni, M. P. *J. Phys. Chem. B* **2003**, *107*, 7492.

(36) Pileni, M. P. *Nat. Mater.* **2003**, *2*, 145.

(37) Lisiecki, I.; Andre, P.; Filankembo, A.; Petit, C.; Tanori, J.; Gulik-Krzywicki, T.; Ninham, B. W.; Pileni, M. P. *J. Phys. Chem.* **1999**, *103*, 9168 and–9176.

(38) Refait, P. H. *J. Mater. Res.* **1993**, *34*, 797.

(39) Olowe, A. A. *J. Mater. Res.* **1991**, *32*, 965.

(40) Shevchenko, E.; Talapin, D.; Kornowski, A. L.; Rogach, A.; Kormowski, A.; Haase, M.; Weller, H. *J. Am. Chem. Soc.* **2002**, *124*, 11480–11485.

JP801632P